

Flavor changing neutrino interactions and CP violation in neutrino oscillations

Toshihiko Hattori,^{a);1} Tsutomu Hasuike,^{b);2} and Seiichi Wakaizumi^{c);3}

^{a)}Institute of Theoretical Physics, University of Tokushima, Tokushima 770-8502, Japan

^{b)}Department of Physics, Anan College of Technology, Anan 774-0017, Japan

^{c)}Center for University Extension, University of Tokushima, Tokushima 770-8502, Japan

Abstract

We investigate the interference effects of non-standard neutrino matter interactions (NSNI) with the mass-induced neutrino oscillations. The NSNI is composed of flavor-changing neutrino interactions (FCNI) and flavor-diagonal neutrino interactions (FDNI). Both of the interactions are introduced in the ν_e sector and the ν_μ sector in order to study their effects in ν_e and ν_μ oscillations, respectively. The FCNI effect proves to possibly dominate the CP violating effect, i.e. the difference between the neutrino and the antineutrino oscillation probabilities. The FCNI effect significantly survives as a fake CP violating effect in the neutrino energy region where the pure CP violating effect, ordinary matter effect and FDNI effect die out, for example, above 4 GeV at the baseline of $L = 730$ km in the ν_e oscillation for the maximum parameter values of FCNI and FDNI allowed by the atmospheric neutrino oscillation data. The FCNI and FDNI effects on the CP violating effect in the ν_e oscillation are negligibly small due to the stringent constraints on FCNI from the bounds on lepton flavor violating processes and on FDNI from the limits on lepton universality violation.

¹e-mail: hattori@ias.tokushima-u.ac.jp

²e-mail: hasuike@anan-nct.ac.jp

³e-mail: wakaizumi@cue.tokushima-u.ac.jp

I Introduction

In the framework of massive neutrinos and leptonic mixing, the atmospheric neutrino anomaly [1] is resolved by the $\nu_\mu \rightarrow \nu_\tau$ oscillation with nearly maximal mixing between ν_μ and ν_τ [2] and the solar neutrino deficit [3] is interpreted by the $\nu_e \rightarrow \nu_\mu$ oscillation with large mixing angle [4] in the Mikheyev-Smirnov-Wolfenstein (MSW) mechanism of neutrino interactions with matter [5] in the three-neutrino scheme, where the neutrino flavor eigenstates ($\nu = e, \mu, \tau$) are expressed by a superposition of their mass eigenstates ν_i ($i = 1, 2, 3$) with mass m_i as follows:

$$\nu = \sum_{i=1}^3 U_{\nu i} \nu_i; \quad (1)$$

where U is the 3×3 unitary mixing matrix, which is called as Maki-Nakagawa-Sakata (MNS) matrix [6]. The reactor experiment of search for ν_e oscillations, CHOOZ, gives an upper limit on the element U_{e3} , which is very small as $|U_{e3}| < 0.22$ [7]. The liquid scintillation experiment, LSND, claims a discovery of $\nu_e \rightarrow \nu_\mu$ oscillations [8], which requires a fourth sterile neutrino.

The above situation seems to convince us of a scheme of massive neutrinos and lepton mixing. In addition to this scheme, it is interesting to investigate non-standard neutrino matter interactions in the neutrino oscillations. The non-standard neutrino matter interaction (NSNI) is originated from Wolfenstein's work [9] and the flavor-changing neutrino matter interaction (FCNI) and flavor-diagonal neutrino matter interaction (FDNI) were used in order to study the solar neutrino problem, not by relying on the mass-induced neutrino oscillations [10][11], and then by considering them as sub-leading effects to the standard mass-induced oscillations [12].

For the atmospheric neutrino problem, the FDNI alone [13] and both of the FCNI and FDNI were applied [14]. The mere NSNI, however, has proved not to be able to solve the atmospheric neutrino problem [15][16]. After that, the FCNI

has been studied as sub-leading effects to the standard mass-induced neutrino oscillations by considering FCNI in μ sector and in e sector [16][17] and its detectability at a future neutrino factory is discussed in Refs.[17][18][19]. In Ref.18, it is shown that the FCNI dominates the e oscillation probability at sufficiently high neutrino energies. There are also combined analyses with the inclusion of new flavor-changing neutrino interactions occurring in the neutrino production and detection processes in addition to the above-mentioned FCNI and FDNI, of which effects are enhanced by the interference with the ordinary weak interactions in the oscillation phenomena [20].

In this paper, we analyze the non-standard neutrino matter interaction effects (NSNI) to the CP violating effects in the neutrino oscillations by considering them in μ sector and e sector in the three-neutrino scheme. The NSNI consists of the above-mentioned FCNI and flavor-diagonal neutrino matter interactions (FDNI). The evolution equation of the neutrino flavor states is solved analytically by using Arifune-Koike-Sato's perturbative method [21] and we calculate the neutrino oscillation probability for the general $\mu \rightarrow e$ oscillation. We apply this analytic expression of the probability to calculate the CP violating effects in $\mu \rightarrow e$ and $e \rightarrow \mu$ oscillations, i.e. the difference between the neutrino and the antineutrino oscillation probabilities. We find that the FCNI matter effect survives and dominates the CP violating effect in $\mu \rightarrow e$ oscillation even after both the pure CP violating effect due to the phase of $U_{e\mu}$ and the fake CP violating ones due to the ordinary and FDNI matter effects die out. This shows that the non-standard flavor changing neutrino matter interaction could be detected in the CP violating effect in $\mu \rightarrow e$ oscillation at the neutrino energies where both the pure CP violating effect and the ordinary matter effect become sufficiently small and undetectable. For $e \rightarrow \mu$ oscillation, the FCNI and FDNI effects on the CP violating effect are negligibly small due to the stringent constraints [11][15][22] on

FCNI from the bounds on lepton flavor violating processes and on FDN I from the limits on lepton universality violation.

The paper is organized as follows. In Sec. II the oscillation probability is derived by solving analytically the evolution equation of the neutrino flavor states with the non-standard neutrino matter interaction in ν_e sector. The effect of the NSNI is studied in the CP violating effects in the ν_e oscillation. In Sect. III the same will be done for the NSNI in ν_μ sector and the effect of the NSNI is studied in the CP violating effects in the ν_μ oscillation. Section IV is devoted to the conclusions and discussions.

II Oscillation probability and CP violating effect with NSNI in ν_e sector

Here and in the next section we calculate the neutrino oscillation probabilities and CP violating effects with the inclusion of the NSNI in ν_e sector and in ν_μ sector, respectively, in the three-neutrino scheme by solving analytically the evolution equation for neutrino flavor states in the perturbative method.

If we consider the effect of NSNI in the ν_e sector, the evolution equation in matter is given as

$$i \frac{d}{dx} \begin{pmatrix} \nu_e^B \\ \nu_e^C \end{pmatrix} = H \begin{pmatrix} \nu_e^B \\ \nu_e^C \end{pmatrix}; \quad (2)$$

and [17]

$$H = \frac{1}{2E} \begin{pmatrix} 0 & 0 & 0 & 1 & 0 & 0 & 0 & 0 & 1 \\ 0 & m_{21}^2 & 0 & U^y & + \frac{B}{E} V_e(x) & 0 & 0 & \frac{f}{E} V_f(x) & 0 \\ 0 & 0 & m_{31}^2 & 0 & 0 & 0 & \frac{f}{E} V_f(x) & \frac{f}{E} V_f(x) & 0 \end{pmatrix}; \quad (3)$$

where E is the neutrino energy, $m_{ij}^2 = m_i^2 - m_j^2$, m_i being the mass of i -th neutrino, U is the MNS leptonic mixing matrix, $V_f(x) = \frac{P}{2G_F n_f(x)}$, x being the position of the running neutrino, $\frac{f}{E} V_f(x)$ is the flavor-changing $+ f!$ $+ f$ forward scattering amplitude due to the flavor-changing neutrino matter interaction (FCNI) and $\frac{f}{E} V_f(x)$ is the flavor-diagonal f elastic forward scattering

amplitude due to the flavor-diagonal neutrino matter interaction (FDNI), with $n_f(x)$ being the number density of the fermion f ($f = u; d; e$) which induces such processes. In Eq.(3), θ^f and ϕ^f are the phenomenological parameters which characterize the strength of FCNI and FDNI, respectively. The fermion number density $n_f(x)$ can be written in terms of the matter density as $n_f(x) = Y_f(x)$, where Y_f is the fraction of the fermion f per nucleon, $Y_e = 1/2$ for electrons and $Y_{u,d} = 1/3$ for u or d quarks. In the following, we consider interactions only with either u or d quarks, since for the NSNI with electrons the same effects presented in this paper can be obtained simply by increasing the parameters $\theta^{u,d}$ and $\phi^{u,d}$ by a factor 3.

For the evolution equation of the antineutrinos, the replacement of $U \rightarrow U^\dagger$; $V_{e,f}(x) \rightarrow V_{e,f}^*(x)$ and $\theta^f \rightarrow \theta^{f*}$ should be done in Eq.(3).

We use here Arafune-Koike-Sato's perturbative method to solve analytically the evolution equation [21]. The solution of Eq.(2) is given by

$$\psi(x) = S(x) \psi(0); \quad (4)$$

with

$$S(x) = T \exp \left[-i \int_0^x ds H(s) \right]; \quad (5)$$

where

$$H(x) = \begin{pmatrix} 0 & 1 \\ \theta^e(x) & \phi^e(x) \end{pmatrix} \quad (6)$$

and T is the time ordering operator. In the following, the oscillation probability and the CP violating effect are calculated for the baseline of $L = 300$ and 730 km so that we assume $n_f(x)$ and $\psi(x)$ to be independent of x . Then we have

$$S(x) = e^{iHx}; \quad (7)$$

The oscillation probability for $\bar{\nu}_e \rightarrow \bar{\nu}_\mu$ at the distance L from the neutrino production point is given in terms of S in Eq.(5) as follows:

$$P(\bar{\nu}_e \rightarrow \bar{\nu}_\mu; L) = |S_{\mu e}(L)|^2; \quad (8)$$

We express the Hamiltonian H of Eq.(3) for simplicity as

$$H = \frac{1}{2E} U \begin{pmatrix} 0 & 0 & 0 \\ 0 & m_{21}^2 & 0 \\ 0 & 0 & m_{31}^2 \end{pmatrix} U^\dagger + \frac{1}{2E} \begin{pmatrix} a & 0 & 0 \\ 0 & 0 & b_A^C \\ 0 & b & b_b^0 \end{pmatrix}; \quad (9)$$

where

$$a = 2E V_e = 2 \frac{p}{2G_F n_e E} = 7.60 \cdot 10^5 \frac{E}{[\text{g cm}^{-3}] [\text{GeV}]} \text{eV}^2; \quad (10)$$

$$b = 2E^\dagger V_f = 15.2 \cdot 10^5 Y_f \frac{E}{[\text{g cm}^{-3}] [\text{GeV}]} \text{eV}^2; \quad (11)$$

$$b_b^0 = 2E^\dagger V_f = 15.2 \cdot 10^5 Y_f^0 \frac{E}{[\text{g cm}^{-3}] [\text{GeV}]} \text{eV}^2; \quad (12)$$

where † and 0 are denoted as † and 0 , respectively, and V_f is denoted as b , for simplicity. In general, † is complex and 0 is real from the hermiticity of the Hamiltonian. Since $m_{21}^2 = m_{31}^2$ and $a; j^\dagger; j^0; b = m_{31}^2$ because of $j^\dagger < 0.04$ and $j^0 < 0.17$ from the analysis of the atmospheric neutrino problem [16], we decompose H of Eq.(9) as $H = H_0 + H_1$ with

$$H_0 = \frac{1}{2E} U \begin{pmatrix} 0 & 0 & 0 \\ 0 & 0 & 0 \\ 0 & 0 & m_{31}^2 \end{pmatrix} U^\dagger; \quad (13)$$

and

$$H_1 = \frac{1}{2E} U \begin{pmatrix} 0 & 0 & 0 \\ 0 & m_{21}^2 & 0 \\ 0 & 0 & 0 \end{pmatrix} U^\dagger + \frac{1}{2E} \begin{pmatrix} a & 0 & 0 \\ 0 & 0 & b_A^C \\ 0 & b & b_b^0 \end{pmatrix}; \quad (14)$$

and treat H_1 as a perturbation and calculate Eq.(7) up to the first order in $m_{21}^2; a; b$ and b_b^0 . Then, $S(x)$ is given by

$$S(x) = e^{iH_0 x} \left[1 + i e^{iH_0 x} \int_0^x ds H_1(s) \right]; \quad (15)$$

where $H_1(x) = e^{iH_0 x} H_1 e^{-iH_0 x}$. The approximation in Eq.(15) requires

$$\frac{m_{21}^2 L}{2E} \ll 1; \quad \frac{j^\dagger L}{2E} \ll 1; \quad \frac{b_b^0 L}{2E} \ll 1; \quad (16)$$

The requirements of Eq.(16) are satisfied for $m_{21}^2 = (10^5 - 10^4) \text{eV}^2; E = 1 - 20 \text{GeV}; L = (300 - 730) \text{km}, \rho = 3 \text{g cm}^{-3}; j^\dagger = 0.03$ and $j^0 = 0.16$ as

$$\frac{m_{21}^2 L}{2E} \ll 4 \cdot 10^4 \cdot 0.2; \quad \frac{j^\dagger L}{2E} \ll (1 - 4) \cdot 10^2;$$

$$\frac{j^0 \mathcal{L}}{2E} \quad (1 \quad 2) \quad 10^1 : \quad (17)$$

Equation (16) also shows that the approximation becomes better as the energy E increases. If we express $S(x)$ as

$$S(x) = \quad + iT(x); \quad (18)$$

then $iT(x)$ is obtained as follows:

$$\begin{aligned} iT(x) = & 2i \exp \left[-i \frac{m_{31}^2 x}{4E} \right] \sin \left[\frac{m_{31}^2 x}{4E} \right] U_{31} U_{31}^\dagger f_1 \left[\frac{a}{m_{31}^2} (2j_{e3}^2) \right. \\ & e^{-i \frac{ax}{2E}} j_{e3}^2 \left. - \frac{b}{m_{31}^2} (2j_{3j}^2) \right] \\ & + i \frac{b x}{2E} j_{3j}^2 g - \frac{1}{m_{31}^2} f_4 U_{31} U_{31}^\dagger \text{Re}(b U_{31} U_{31}^\dagger) \\ & + b(U_{31} U_{31}^\dagger + U_{31} U_{31}^\dagger) + b(U_{31} U_{31}^\dagger \\ & + U_{31} U_{31}^\dagger) g - 2i \frac{x}{2E} U_{31} U_{31}^\dagger \text{Re}(b U_{31} U_{31}^\dagger) \\ & + i \frac{m_{31}^2 x^h}{2E} \frac{m_{21}^2}{m_{31}^2} U_{21} U_{21}^\dagger + \frac{a}{m_{31}^2} f_e e^{-i \frac{ax}{2E}} + U_{31} U_{31}^\dagger (2j_{e3}^2) e \\ & e) g + \frac{b}{m_{31}^2} f_e + U_{31} U_{31}^\dagger (2j_{3j}^2) g \\ & + \frac{1}{m_{31}^2} f_b + b + 4U_{31} U_{31}^\dagger \text{Re}(b U_{31} U_{31}^\dagger) \\ & + b(U_{31} U_{31}^\dagger + U_{31} U_{31}^\dagger) + b(U_{31} U_{31}^\dagger \\ & + U_{31} U_{31}^\dagger) g : \quad (19) \end{aligned}$$

We use Eq.(19) in Eq.(18) and calculate the oscillation probability for $\nu_\mu \rightarrow \nu_\tau$ by Eq.(8). The complete expression of $P(\nu_\mu \rightarrow \nu_\tau; L)$ with the NSNI in the sector is given in the Appendix A.

Now we will study the effects due to the NSNI in the $\nu_\mu \rightarrow \nu_\tau$ sector on the oscillation probability and the CP violating effect in $\nu_\mu \rightarrow \nu_\tau$ oscillation at the baseline of $L = 730$ km. For the MNS mixing matrix U , we take the standard parametrization given by

$$U = \begin{pmatrix} 1 & 0 & 0 \\ 0 & c_{12} c_{13} & s_{12} c_{13} & s_{13} e^{-i\delta} \\ 0 & s_{12} c_{23} - c_{12} s_{23} s_{13} e^{i\delta} & c_{12} c_{23} - s_{12} s_{23} s_{13} e^{i\delta} & s_{23} c_{13} \\ 0 & s_{12} s_{23} + c_{12} c_{23} s_{13} e^{i\delta} & c_{12} s_{23} + s_{12} c_{23} s_{13} e^{i\delta} & c_{23} c_{13} \end{pmatrix} \quad (20)$$

where $c_{ij} = \cos \theta_{ij}$; $s_{ij} = \sin \theta_{ij}$ and δ is the CP violating phase. From the Super-Kamiokande data for the atmospheric neutrino oscillation [2], $\sin^2 2\theta_{atm} > 0.82$ and $5 \times 10^4 < m_{atm}^2 < 6 \times 10^3 \text{ eV}^2$, we take in the following $\sin \theta_{23} = 0.742$ for the mixing angle s_{23} and $m_{31}^2 = 2.5 \times 10^3 \text{ eV}^2$ as a typical value. For s_{12} , we take $\sin \theta_{12} = 0.541$ and $m_{21}^2 = 5 \times 10^5 \text{ eV}^2$ from the presently most probable large-mixing angle solution (LMA) to the solar neutrino oscillation [23]. For s_{13} , we tentatively assume $\sin \theta_{13} = 0.16$ from the CHOOZ data on ν_e oscillation [7], $\sin^2 2\theta_{CHOOZ} < 0.18$ for $3 \times 10^3 < m^2 < 1.0 \times 10^2 \text{ eV}^2$, which means $0 < \sin \theta_{13} < 0.22$. For the phenomenological parameters of the NSNI, the constraints are derived to be $0.05 < \epsilon < 0.04$ and $|\eta_j| < 0.17$ from the analyses of the atmospheric neutrino data by Fonengo et al. [16]. They assumed δ to be real. Here we generally take δ to be complex. For the numerical calculations we take $\eta_j = 0.03$ and $\delta = 0.16$, and the effects of the FCNI on CP violation has proved to be maximum at $\delta = 0$ and $\delta = \pi$ for the phase of δ , $\delta = \eta_j \delta_e$.

In the following, we present the numerical results for the oscillation probabilities and CP violating effects in the $\nu_\mu \rightarrow \nu_\tau$ oscillation. The effect of NSNI in the $\nu_\mu \rightarrow \nu_\tau$ sector is not so significant in the $\nu_\mu \rightarrow \nu_e$ and $\nu_e \rightarrow \nu_\tau$ oscillations as in the $\nu_\mu \rightarrow \nu_\tau$ oscillation. Fig.1 and Fig.2 show the $\nu_\mu \rightarrow \nu_\tau$ oscillation probabilities for $\eta_j = 0.03$; $\delta = 0$; $\delta = 0.16$; $\delta = \pi$; $m_{31}^2 > 0$ for the neutrino energy range of $E = 0.1 \sim 1 \text{ GeV}$ and $E = 1 \sim 20 \text{ GeV}$, respectively, at the baseline of $L = 730 \text{ km}$, where the solid line represents the oscillation probability including all the three matter effects, i.e. ordinary matter effect (denoted as a in Eq.(14)),avor-changing neutrino matter interaction (FCNI, denoted as b) and avor-diagonal neutrino matter interaction (FDNI, denoted as δ^0 b), and the dashed line represents the one without any matter effects. Fig.3 shows the oscillation probabilities for $\delta = \pi$ with the same values of η_j and δ^0 as in Figs.1 and 2. These three Figures show that the matter effects due to the NSNI are small on the oscillation

probability.

Figs.4-9 show the CP violating effects in the $\nu_e \rightarrow \nu_\mu$ oscillation, calculated as the difference between the neutrino and the antineutrino oscillation probabilities, for the energy range of $E = 1 - 20$ GeV at the baseline of $L = 730$ km. The phase of the MNS mixing matrix U is taken as $\delta = \pi/2$. The dash-dotted line is the pure CP violating effect due to the phase of U . The long-dashed, short-dashed and dotted lines are the fake CP violating effects due to the ordinary, FCNI and FDNImatter effects, respectively. The solid line represents the total CP violating effect with the sum of the pure and fake ones. In Figs.6-8, the FDN I contribution is not drawn, since it is of the same magnitude as in Figs.4-5 apart from its sign. For Figs.4-8, we have taken $\theta_{12} = 0.03$; $\theta_{13} = 0.16$ and $\theta_{23} = 2.5 \times 10^{-3}$ eV². In Fig.4, the phase of θ_{13} is taken as $\delta_{13} = 0$ and $\delta_{23} = +0.16$ (> 0) and $m_{31}^2 > 0$. In Fig.5, $\delta_{13} = 0$; $\delta_{23} = 0.16$ (< 0) and $m_{31}^2 > 0$. In Fig.6, $\delta_{13} = \pi$; $\delta_{23} > 0$ and $m_{31}^2 > 0$. In Fig.7, $\delta_{13} = 0$; $\delta_{23} > 0$ and $m_{31}^2 < 0$ and in Fig.8, $\delta_{13} = \pi$; $\delta_{23} > 0$ and $m_{31}^2 < 0$. As can be seen from these figures, the FCNI matter effect dominates the CP violating effect in the whole range of $E = 1 - 20$ GeV, and all the other contributions of pure CP violation, ordinary matter effect and FDN I effect rapidly die out around 4 GeV and the FCNI effect survives significantly above this energy. When the sign of m_{31}^2 is changed, the contributions of all the matter effects including FCNI and FDN I change the sign, as can be seen from the comparison of Fig.4 and Fig.7. In Fig.9 the pure and fake CP violating effects are shown for the smaller θ_{13} and θ_{23} values, $\theta_{12} = 0.01$; $\delta_{13} = 0$ and $\delta_{23} = 0.01$.

Next we show in Figs.10-11 the effects of NSNI in the CP violating effect in $\nu_e \rightarrow \nu_\mu$, which is the difference of $\nu_e \rightarrow \nu_\mu$ and $\bar{\nu}_e \rightarrow \bar{\nu}_\mu$ survival probabilities. The long-dashed, short-dashed and dotted lines represent the ordinary, FCNI and FDNImatter effects, respectively, and the solid line does the total CP violating effect. In Fig.10 we give the CP violating effects in the energy range of $E = 0.3 - 2$

GeV at the baseline of $L = 300$ km for $\theta_{12} = 0.03$; $\theta_{13} = 0$; $\theta_{23} = 0.16$, and $m_{31}^2 > 0$. The ordinary matter effect and the FDNI effect are very small and the FCNI effect dominates above 0.8 GeV. In Fig.11, we give the CP violating effect in $\nu_e \rightarrow \nu_e$ in the energy range of $E = 0.5 \sim 3.0$ GeV at the baseline of $L = 730$ km for $\theta_{12} = 0.03$; $\theta_{13} = 0$; $\theta_{23} = 0.16$, and $m_{31}^2 > 0$. Again, the ordinary matter effect and the FDNI effect are very small and the FCNI effect dominates above 1 GeV.

III NSNI in ν_e sector

In this section, we consider the NSNI in ν_e sector and study its effect on the oscillation probability and CP violating effect in ν_e oscillation at the baselines of $L = 300$ km.

The Hamiltonian of the evolution equation of the flavor neutrino states is given as

$$H = \frac{1}{2E} U \begin{pmatrix} 0 & 0 & 0 \\ 0 & m_{21}^2 & 0 \\ 0 & 0 & m_{31}^2 \end{pmatrix} U^\dagger + \begin{pmatrix} 0 & V_e(x) & 0 \\ V_e^*(x) & 0 & 0 \\ 0 & 0 & 0 \end{pmatrix} + \begin{pmatrix} 0 & V_f(x) & 0 \\ V_f^*(x) & 0 & 0 \\ 0 & 0 & 0 \end{pmatrix}; \quad (21)$$

where $V_e(x)$ is the flavor-changing $\nu_e + \nu_e \rightarrow \nu_e + \nu_e$ forward scattering amplitude due to the FCNI and $V_f(x)$ is the flavor-diagonal ν_e elastic forward scattering amplitude due to the FDNI. As in the previous section, we assume the matter density to be constant for the baseline of $L = 300$ and 730 km and reexpress Eq.(21) as

$$H = \frac{1}{2E} U \begin{pmatrix} 0 & 0 & 0 \\ 0 & m_{21}^2 & 0 \\ 0 & 0 & m_{31}^2 \end{pmatrix} U^\dagger + \frac{1}{2E} \begin{pmatrix} a & b & 0 \\ b & 0 & 0 \\ 0 & 0 & 0 \end{pmatrix}; \quad (22)$$

where a is the same as in Eq.(10) and

$$b = 2E V_e^* V_f = 15.2 \times 10^5 Y_f \frac{E}{[\text{g cm}^{-3}] [\text{GeV}]} \text{eV}^2; \quad (23)$$

$$0b = 2E V_f^* V_f = 15.2 \times 10^5 Y_f^0 \frac{E}{[\text{g cm}^{-3}] [\text{GeV}]} \text{eV}^2; \quad (24)$$

where V_e^* and V_f^* are denoted as a and 0 , respectively, and V_f is denoted as b , for simplicity. In general, a is complex and 0 is real. The experimental limits

on various lepton flavor violating processes and $SU(2)_L$ breaking effects give a stringent constraint on the FCNI parameter as $j_j < 7 \times 10^5$ [11][15][22] and the upper bounds on lepton universality violation give a constraint on the FDMI parameter as $j_j^0 < 0.1$ [11][15]. So, we can decompose H of Eq.(22) as $H = H_0 + H_1$ with

$$H_1 = \frac{1}{2E} U \begin{pmatrix} 0 & 0 & 0 \\ 0 & m_{21}^2 & 0 \\ 0 & 0 & 0 \end{pmatrix} U^\dagger + \frac{1}{2E} \begin{pmatrix} 0 & a & b \\ 0 & b & 0 \\ 0 & 0 & 0 \end{pmatrix}; \quad (25)$$

and treat H_1 as a perturbation. H_0 is the same as in Eq.(13). In the same way as for the NSNI in ν_e sector, we calculate $S(x)$ of Eq.(7) up to the first order in m_{21}^2/a ; b and b_0 to obtain the expression of $iT(x)$ in Eq.(18):

$$\begin{aligned} iT(x) = & 2i \exp\left[-i \frac{m_{31}^2 x}{4E}\right] \sin\left[\frac{m_{31}^2 x}{4E}\right] U_3 U_3^\dagger \left[\frac{a}{m_{31}^2} (2J_{e3}^2) \right. \\ & \left. - \frac{ax}{2E} J_{e3}^2 - \frac{b_0}{m_{31}^2} (2J_{33}^2) \right] \\ & - \frac{b_0 x}{2E} J_{33}^2 g - \frac{1}{m_{31}^2} f 4U_3 U_3^\dagger \text{Re}(b U_{e3} U_3) \\ & + b(U_3 U_{e3} + U_3 U_3^\dagger) - b(U_3 U_3^\dagger + U_3 U_{e3}) \\ & + U_3 U_{e3} \Big) g - 2i \frac{x}{2E} U_3 U_3^\dagger \text{Re}(b U_{e3} U_3) \\ & + \frac{m_{31}^2 x}{2E} \frac{m_{21}^2}{m_{31}^2} U_2 U_2^\dagger + \frac{a}{m_{31}^2} f (e_e + U_3 U_3^\dagger) (2J_{e3}^2) \\ & + \frac{b_0}{m_{31}^2} f (e_e + U_3 U_3^\dagger) (2J_{33}^2) g \\ & + \frac{1}{m_{31}^2} f (b_e + b_e + 4U_3 U_3^\dagger \text{Re}(b U_{e3} U_3) \\ & + b(U_3 U_{e3} + U_3 U_3^\dagger) - b(U_3 U_3^\dagger + U_3 U_{e3}) \\ & + U_3 U_{e3} \Big) g : \quad (26) \end{aligned}$$

Using Eq.(26) in Eq.(18), we calculate the oscillation probability for $\nu_e \rightarrow \nu_e$ by Eq.(8). The complete expression of $P(\nu_e \rightarrow \nu_e; L)$ with the NSNI in ν_e sector is given in the Appendix B.

Now we will study the effects due to the NSNI in ν_e sector on the CP violating effect in $\nu_e \rightarrow \nu_e$ oscillation at the baseline of $L = 300$ km. The values

of the parameters m_{21}^2 ; m_{31}^2 ; s_{23} ; s_{12} and s_{13} are taken to be the same as in the previous section. The effect of the FCNI on CP violation has proved to be maximum at $\theta = \pi/2$ and $3\pi/2$ for the phase of δ ; $\delta = j\pi$. We present the numerical results for the CP violating effects in the ν_e oscillation for the case of parameters not satisfying the constraints, $j = 0.10$ and 0.03 , and for the case of parameters satisfying the constraints, $j = 7 \times 10^5$. In Fig.12 and Fig.13, we show the CP violating effect in ν_e oscillation for $j = 0.10$; $\theta = \pi/2$; $\delta = 0.10$ and for $j = 0.03$; $\theta = \pi/2$; $\delta = 0.03$, respectively, in the neutrino energy range of $E = 0.3 - 2$ GeV at the baseline of $L = 300$ km for $m_{31}^2 > 0$ and $\theta = \pi/2$ for the phase of U . The dash-dotted line represents the pure CP violating effect due to the phase of U . The long-dashed, short-dashed and dotted lines are the fake CP violating effects due to the ordinary, FCNI and FDNImatter effects, respectively. The solid line represents the total CP violating effect, which is the sum of the pure and fake ones. The contribution of the FDNImatter effect has proved to be remarkably small. The pure CP violating effect and the fake CP violating one due to the ordinary matter effect rapidly die out around 1.4 GeV, while the contribution of the FCNI effect survives significantly above this energy. Especially, the FCNI effect dominates the CP violating effect above 1 GeV for the case of $j = 0.10$ and $\delta = 0.10$, as can be seen in Fig.12. In Fig.14, the CP violating effects are shown for $j = 7 \times 10^5$ and $\delta = 0.01$, which are in the stringent constraint range on j obtained from the lepton flavor violating processes and $SU(2)_L$ violation. The dash-dotted, long-dashed and short-dashed lines represent the pure CP violating effect, the fake CP violating ones due to the ordinary and FCNI matter effects, respectively. The solid line represents the total CP violating effect. The FCNI effect turns out to be negligibly small, so that the total CP violating effect is just given by the pure CP violating effect and the ordinary matter effect. The FDNImatter effect is negligibly small just as the FCNI effect and is not shown in Fig.14.

IV Conclusions and discussions

In this paper we have studied the effect of non-standard neutrino matter interactions on the standard mass-induced oscillation probabilities and the CP violating effects. The non-standard interactions are introduced in the flavor-changing neutrino interaction (FCNI) and the flavor-diagonal one (FDNI) as sub-leading effects in the ν_μ sector and ν_e sector in order to investigate their effects in $\nu_\mu \rightarrow \nu_\mu$ and $\nu_\mu \rightarrow \nu_e$ oscillations, respectively, at the baselines of $L = 730$ and 300 km. In $\nu_\mu \rightarrow \nu_\mu$ oscillation at $L = 730$ km, the FCNI contribution dominates and survives significantly above the neutrino energy 4 GeV, where all the others of pure CP violating effect, ordinary matter effect and FDNI contribution die out. In $\nu_\mu \rightarrow \nu_e$ oscillation at $L = 300$ km, the FCNI and FDNI contributions are negligibly small due to the stringent constraints on FCNI from the bounds on various lepton flavor violating processes and on FDNI from the limits on lepton universality violation.

These results show that the non-standard neutrino matter interactions, especially the flavor-changing neutrino interaction, could be detected in the CP violating effect in $\nu_\mu \rightarrow \nu_\mu$ oscillation at the neutrino energies where both the pure CP violating effect and the ordinary matter effect die out, for example, above 4 GeV at $L = 730$ km. The FCNI effect might also be detected in the difference between $\nu_\mu \rightarrow \nu_\mu$ and $\nu_\mu \rightarrow \nu_e$ oscillation probabilities in 0.8 - 2 GeV for the baseline of $L = 300$ km and above 2 GeV for the baseline of $L = 730$ km.¹

¹After the completion of this work, Prof. Branco informed us that they studied the effect of the addition of a new isosinglet charged lepton inspired by extra dimensions to the standard spectrum on the CP asymmetries in neutrino oscillations in ν_e and ν_μ channels and its detectability at future neutrino factories. [24]

Appendix A : Oscillation probability
with NSNI in θ sector

Here we present the oscillation probability of Eq.(8) with Eq.(19) taken in Eq.(18).

$$\begin{aligned}
 P(\nu_\mu \rightarrow \nu_\tau; L) &= \frac{1}{4} \sin^2 \frac{m_{31}^2 L}{4E} \left[1 - 2 \frac{a}{m_{31}^2} (\nu_{e3} \nu_e) \right. \\
 &\quad \left. - 2 \frac{b}{m_{31}^2} (\nu_{3\mu} \nu_\mu) \right] + \frac{2}{m_{31}^2} \text{Re}(b U_{3\mu} U_{3\tau}) (2 \nu_{3\mu} \nu_\mu) \\
 &\quad + 2 \sin^2 \frac{m_{31}^2 L}{2E} \nu_{3\mu} \nu_\mu \frac{aL}{2E} \nu_{e3} \nu_e + 2 \frac{L}{2E} \text{Re}(b U_{3\mu} U_{3\tau}) + \frac{bL}{2E} \nu_{3\mu} \nu_\mu \\
 &+ 4 \sin^2 \frac{m_{31}^2 L}{4E} \nu_{3\mu} \nu_\mu \nu_{3\tau} \nu_\tau \left[1 - 2 \frac{a}{m_{31}^2} (2 \nu_{e3} \nu_e) \right. \\
 &\quad \left. - 2 \frac{b}{m_{31}^2} (2 \nu_{3\mu} \nu_\mu) \right] + \frac{2}{m_{31}^2} \text{Re}(b U_{3\mu} U_{3\tau}) f_{4\nu_{3\mu} \nu_\mu \nu_{3\tau} \nu_\tau} \\
 &\quad + \nu_{3\mu} \nu_\mu (\dots) + \nu_{3\tau} \nu_\tau (\dots) g + 2 \frac{m_{31}^2 L}{2E} \sin^2 \frac{m_{31}^2 L}{2E} \\
 &\quad + \frac{m_{21}^2}{m_{31}^2} \text{Re}(U_{3\mu} U_{2\mu} U_{3\tau} U_{2\tau}) + \frac{a}{m_{31}^2} f_{e\tau} \nu_{e3} \nu_e + \nu_{3\mu} \nu_\mu \nu_{3\tau} \nu_\tau (2 \nu_{e3} \nu_e) \\
 &\quad + \frac{b}{m_{31}^2} f_{\nu_{3\mu} \nu_\mu} + \nu_{3\mu} \nu_\mu \nu_{3\tau} \nu_\tau (2 \nu_{3\mu} \nu_\mu) g \\
 &+ \frac{1}{m_{31}^2} \text{Re}(b U_{3\mu} U_{3\tau}) f_{\nu_{3\mu} \nu_\mu} + \dots + 4 \nu_{3\mu} \nu_\mu \nu_{3\tau} \nu_\tau \\
 &\quad + \nu_{3\mu} \nu_\mu (\dots) + \nu_{3\tau} \nu_\tau (\dots) g + 4 \frac{m_{31}^2 L}{2E} \sin^2 \frac{m_{31}^2 L}{4E} \\
 &\quad + \frac{m_{21}^2}{m_{31}^2} \text{Im}(U_{3\mu} U_{2\mu} U_{3\tau} U_{2\tau}) + \frac{1}{m_{31}^2} \text{Im}(b U_{3\mu} U_{3\tau}) f_{\nu_{3\mu} \nu_\mu} \\
 &+ \nu_{3\mu} \nu_\mu (\dots) + \nu_{3\tau} \nu_\tau (\dots) g : \tag{A1}
 \end{aligned}$$

Appendix B : Oscillation probability
with NSNI in ν_e sector

Here we present the oscillation probability of Eq.(8) with Eq.(26) taken in Eq.(18).

$$\begin{aligned}
 P(\nu_e \rightarrow \nu_e; L) &= \frac{1}{4} \sin^2 \frac{m_{31}^2 L}{4E} \left[1 - 2 \frac{a}{m_{31}^2} (\nu_{e3} \nu_e) \right. \\
 &\quad \left. - 2 \frac{b}{m_{31}^2} (\nu_{32} \nu_e) \right] + \frac{2}{m_{31}^2} \text{Re}(\nu_{e3} \nu_{32}) (2\nu_{32} \nu_e)^{\circ} \\
 &\quad + 2 \sin^2 \frac{m_{31}^2 L}{2E} \nu_{32} \nu_e \frac{aL}{2E} \nu_{e3} \nu_e + 2 \frac{L}{2E} \text{Re}(\nu_{e3} \nu_{32}) + \frac{bL}{2E} \nu_{32} \nu_e^{\circ} \\
 &+ 4 \sin^2 \frac{m_{31}^2 L}{4E} \nu_{32} \nu_e \nu_{32} \nu_e \left[1 - 2 \frac{a}{m_{31}^2} (2\nu_{e3} \nu_e) \right. \\
 &\quad \left. - 2 \frac{b}{m_{31}^2} (2\nu_{32} \nu_e) \right] + \frac{2}{m_{31}^2} \text{Re}(\nu_{e3} \nu_{32}) f_4 \nu_{32} \nu_e \nu_{32} \\
 &\quad \nu_{32} \nu_e (\nu_e + \nu_e) \nu_{32} \nu_e (\nu_e + \nu_e) g + 2 \frac{m_{31}^2 L}{2E} \sin^2 \frac{m_{31}^2 L}{2E} \\
 &\quad + \frac{m_{21}^2}{m_{31}^2} \text{Re}(\nu_{32} \nu_{23} \nu_{32} \nu_{23}) + \frac{a}{m_{31}^2} f_e \nu_e \nu_{e3} \nu_e + \nu_{32} \nu_e \nu_{32} (2\nu_{e3} \nu_e \\
 &\quad \nu_e) g + \frac{b}{m_{31}^2} f_e \nu_{32} \nu_e + \nu_{32} \nu_e \nu_{32} (2\nu_{32} \nu_e) g \\
 &+ \frac{1}{m_{31}^2} \text{Re}(\nu_{e3} \nu_{32}) f_e + \nu_e + 4 \nu_{32} \nu_e \nu_{32} \\
 &\quad \nu_{32} \nu_e (\nu_e + \nu_e) \nu_{32} \nu_e (\nu_e + \nu_e) g + 4 \frac{m_{31}^2 L}{2E} \sin^2 \frac{m_{31}^2 L}{4E} \\
 &\quad + \frac{m_{21}^2}{m_{31}^2} \text{Im}(\nu_{32} \nu_{23} \nu_{32} \nu_{23}) + \frac{1}{m_{31}^2} \text{Im}(\nu_{e3} \nu_{32}) f_e \\
 &\quad + \nu_{32} \nu_e (\nu_e) \nu_{32} \nu_e (\nu_e) g : \tag{B1}
 \end{aligned}$$

References

- [1] Kamioke Collaboration, K. S. Hirata et al., *Phys. Lett. B* 205, 416 (1988);
Kamioke Collaboration, Y. Fukuda et al., *Phys. Lett. B* 335, 237 (1994);
IMB Collaboration, D. Casper et al., *Phys. Rev. Lett.* 66, 2561 (1991);
IMB Collaboration, R. Becker-Szendy et al., *Phys. Rev. D* 46, 3720 (1992);
Soudan2 Collaboration, W. W. M. Allison et al., *Phys. Lett. B* 391, 491 (1997);
449, 137 (1999); Super-Kamioke Collaboration, Y. Fukuda et al., *Phys.*
Lett. B 433, 9 (1998); 436, 33 (1998); *Phys. Rev. Lett.* 82, 2644 (1999);
MACRO Collaboration, M. Ambrosio et al., *Phys. Lett. B* 434, 451 (1998);
478, 5 (2000).
- [2] Super-Kamioke Collaboration, Y. Fukuda et al. *Phys. Rev. Lett.* 81, 1562
(1998).
- [3] Homestake Collaboration, B. T. Cleveland et al., *Astrophys. J.* 496, 505
(1988); K. Lande et al., *Nucl. Phys. B (Proc. Suppl.)* 91, 50 (2001); SAGE
Collaboration, J. N. Abdurashitov et al., *Phys. Rev. C* 60, 055801 (1999);
GALLEX Collaboration, W. Hampe et al., *Phys. Lett. B* 447, 127 (1999);
GNO Collaboration, M. Altmann et al., *Phys. Lett. B* 490, 16 (2000);
Kamioke Collaboration, Y. Fukuda et al., *Phys. Rev. Lett.* 77, 1683
(1996); Super-Kamioke Collaboration, Y. Fukuda et al., *Phys. Rev. Lett.*
81, 1158 (1998); *Erratum* 81, 4279 (1998); 82, 1810 (1999); 82, 2430 (1999);
Super-Kamioke Collaboration, S. Fukuda et al., *Phys. Rev. Lett.* 86, 5651
(2001); SNO Collaboration, Q. R. Ahmad et al., *Phys. Rev. Lett.* 87, 071301
(2001); 89, 011301 (2002); 89 011302 (2002).
- [4] J. N. Bahcall, P. I. Krastev, and A. Yu. Smirnov, *Phys. Rev. D* 58, 096016
(1998); G. Fogli, E. Lisi, D. Montanino, and A. Palazzo, *ibid.* 62, 013002
(2000); 64, 093007 (2001); J. N. Bahcall, M. C. Gonzalez-Garcia, and C. Pena-

- G aray, JHEP 0108, 014 (2001); A .Bandyopadhyay, S.C houbey, S.G oswami, and K .K ar, Phys. Lett. B 519, 83 (2001).
- [5] S.P .M ikheyev and A .Yu. Sm imov, Sov. J. Nucl. Phys. 42, 913 (1985); Nuovo C imento C 9, 17 (1986); L. W olfenstein, Phys. Rev. D 17, 2369 (1978).
- [6] Z. M aki, M .Nakagawa, and S. Sakata, Prog. Theor. Phys. 28, 870 (1962).
- [7] M .Apollonio et al., Phys. Lett. B 420, 397 (1998); 466, 415 (1999).
- [8] C .A thanassopoulos et al., Phys. Rev. Lett. 75, 2650 (1995); 77, 3082 (1996); 81, 1774 (1998); R.L. Im lay (LSND Collaboration), in ICHEP 2000, Proceedings of the 30th International Conference on High Energy Physics, Osaka, July 2000, eds. C.S. Lim and T. Yam anaka, p950.
- [9] W olfenstein [3]; L. W olfenstein, Phys. Rev. D 20, 2634 (1979).
- [10] J.W .F. Valle, Phys. Lett. B 199, 432 (1987); M .Fukugita and T. Yanagida, Phys. Lett. B 206, 93 (1988); M .M .G uzzo, A .M asiero, and S.T .P etcov, Phys. Lett. B 260, 154 (1991); E. Roulet, Phys. Rev. D 44, 935 (1991); V .Barger, R.J.N .Phillips, and K .W hisnant, Phys. Rev. D 44, 1629 (1991).
- [11] S. Bergm ann, M .M .G uzzo, P.C .de Holanda, P.I. Krastev, and H .Nunokawa, Phys. Rev. D 62, 073001 (2000).
- [12] S. Bergm ann, Nucl. Phys. B 515, 363 (1998); Z. Berezhiani, R.S. Raghavan, and A .Rossi, Nucl. Phys. B 638, 62 (2002).
- [13] E. M a and P. Roy, Phys. Rev. Lett. 80, 4637 (1998).
- [14] M .C .G onzalez-G arcia, M .M .G uzzo, P.I. Krastev, H .Nunokawa, O.L.G .Peres, V .P leitez, J.W .F. Valle, and R. Zukanovich Funchal, Phys. Rev. Lett. 82, 3202 (1999); P. Lipari and M .Lusignoli, Phys. Rev. D 60, 013003

- (1999); N. Fomenko, M. C. Gonzalez-Garcia, and J. W. F. Valle, JHEP 0007, 006 (2000).
- [15] S. Bergmann, Y. Grossman, and D. M. Pierce, Phys. Rev. D 61, 053005 (2000).
- [16] N. Fomenko, M. Maltoni, R. Tomas Bayo, and J. W. F. Valle, Phys. Rev. D 65, 013010 (2001).
- [17] A. M. Gago, M. M. Guzzo, H. Nunokawa, W. J. C. Teves, and R. Zukanovich Funchal, Phys. Rev. D 64, 073003 (2001).
- [18] P. Huber and J. W. F. Valle, Phys. Lett. B 523, 151 (2001); P. Huber, T. Schwetz, and J. W. F. Valle, Phys. Rev. Lett. 88, 101804 (2002).
- [19] M. Campanelli and A. Romanino, hep-ph/0207350.
- [20] M. C. Gonzalez-Garcia, Y. Grossman, A. Gusso, and Y. Nir, Phys. Rev. D 64, 096006 (2001); T. Ota, J. Sato, and N. Yamashita, Phys. Rev. D 65, 093015 (2002); P. Huber, T. Schwetz, and J. W. F. Valle, Phys. Rev. D 66, 013006 (2002).
- [21] J. Arafa, M. Koike, and J. Sato, Phys. Rev. D 56, 3093 (1997); 60, 119905 (E) (1999).
- [22] S. Bergmann and Y. Grossman, Phys. Rev. D 59, 093005 (1999).
- [23] Super-Kamiokande Collaboration, S. Fukuda et al. Phys. Rev. Lett. 86, 5656 (2001).
- [24] G. C. Branco, D. D. Delpine, B. Nobre, and J. Santiago, hep-ph/0209263.

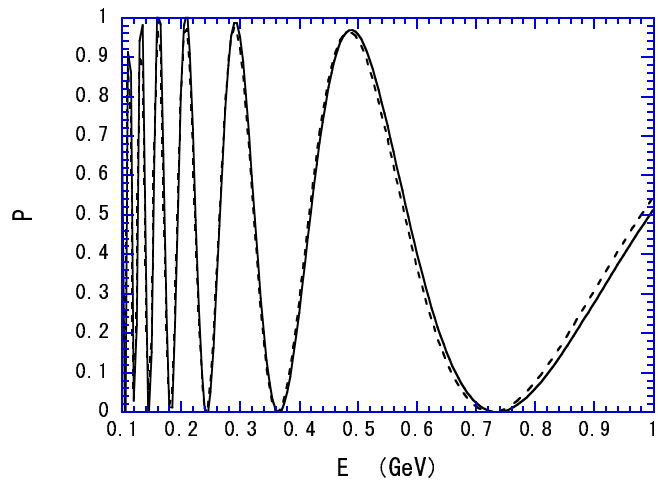


Figure 1: μ oscillation probability for the neutrino energy range $E = 0.1 - 1$ GeV at the baseline of $L = 730$ km, with the NSNI in μ sector. The solid line is the one with all of the ordinary, FCNI and FDMI matter effects included for $\theta_{12} = 0.03$; $\theta_{13} = 0.16$; $\delta = 0$ for the phase of θ_{12} , $\delta = \pi/2$ for the phase of θ_{13} ; $m_{21}^2 = 5 \times 10^5$ eV², and $m_{31}^2 = 2.5 \times 10^3$ eV² (> 0). The dashed line is the one without any matter effects.

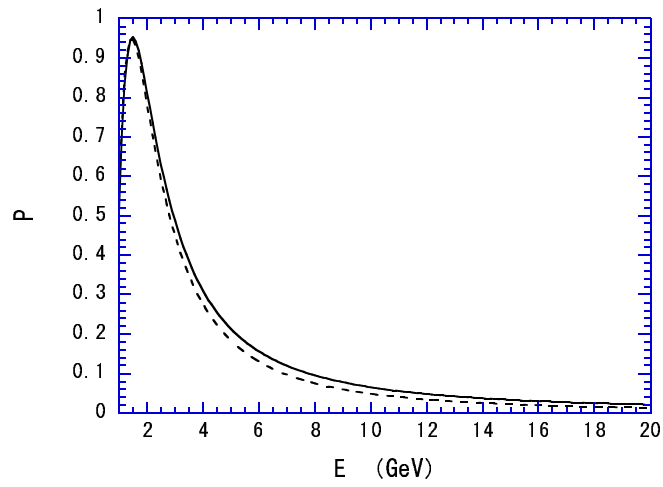


Figure 2: ν_e oscillation probability for the neutrino energy range $E = 1 - 20$ GeV at $L = 730$ km with all of the ordinary, FCNI and FDNI matter effects included (solid line) and without any matter effects (dashed line). The parameter values are the same as in Fig.1.

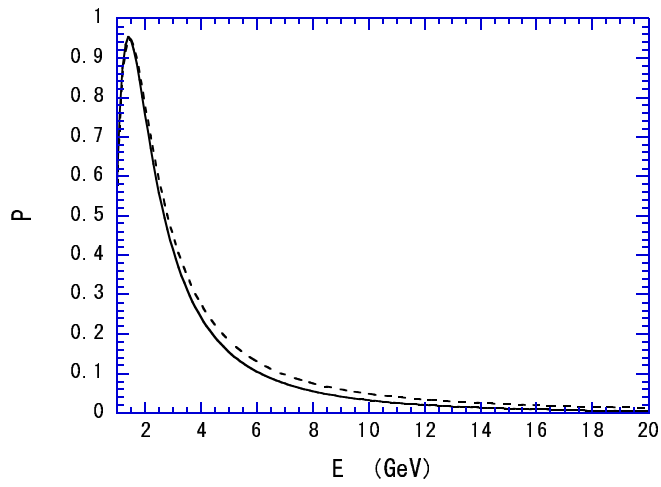


Figure 3: $\nu_e \rightarrow \nu_\mu$ oscillation probability for the neutrino energy range $E = 1 - 20$ GeV at $L = 730$ km with all of the ordinary, FCNI and FDNI matter effects included (solid line) and without any matter effects (dashed line). The parameter values are the same as in Fig.1 except for $\theta_{13} = 0$.

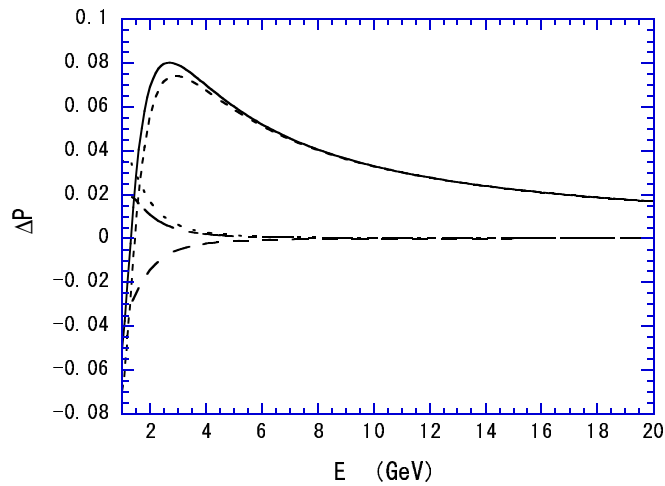


Figure 4: The CP violating effect in $\nu_e \rightarrow \nu_\mu$ oscillation for the neutrino energy range $E = 1 - 20$ GeV at $L = 730$ km, with the NSNI in the ν_e sector. The dash-dotted line is the pure CP violating effect. The long-dashed, short-dashed and dotted lines are the fake CP violating effects due to the ordinary, FCNI and FDNI matter effects, respectively. The solid line is the total CP violating effect with the pure and fake ones. The parameter values are $\theta_{12} = 0.03$; $\theta_{13} = 0.16$; $\delta = 0$; $s_{12} = 0.541$; $s_{23} = 0.742$; $s_{13} = 0.16$; $\sigma = -2$; $m_{21}^2 = 5 \times 10^5 \text{ eV}^2$, and $m_{31}^2 = 2.5 \times 10^3 \text{ eV}^2 (> 0)$.

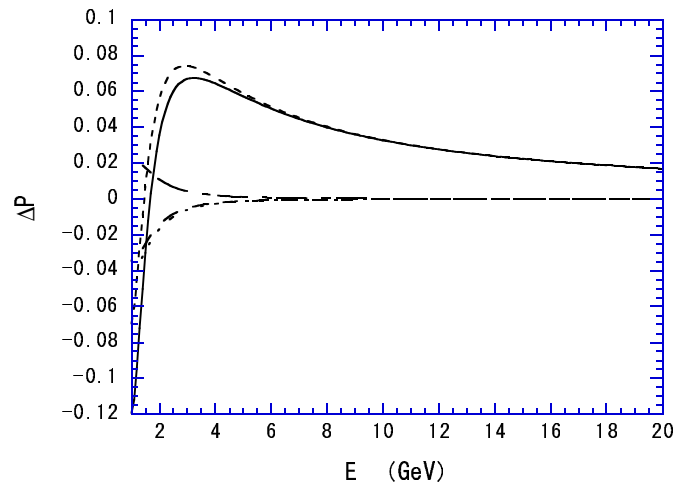


Figure 5: The CP violating effect in $\mu \rightarrow e \gamma$ oscillation at $L = 730$ km with the same parameter values as in Fig.4 except for $\theta_{12} = 0.16$. The lines represent the same ones as in Fig.4. The FDN I contribution changes the sign as compared with the one in Fig.4.

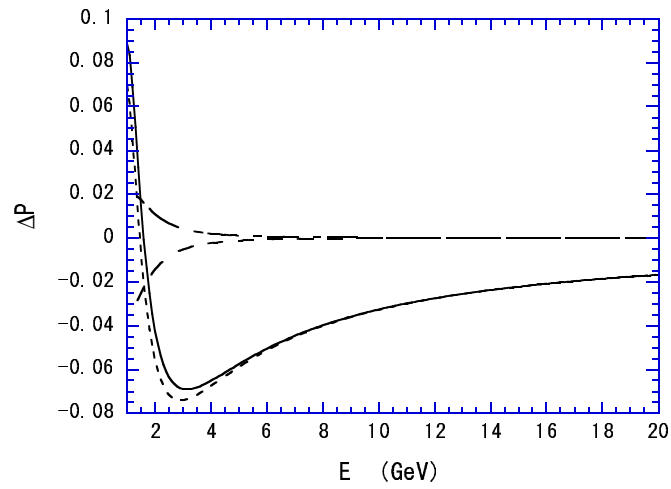


Figure 6: The CP violating effect in $\nu_\mu \rightarrow \nu_\tau$ oscillation at $L = 730$ km with the same parameter values as in Fig.4 except for $\theta_{13} = 0$. The lines represent the same ones as in Fig.4 except for the line of FDN I contribution omitted.

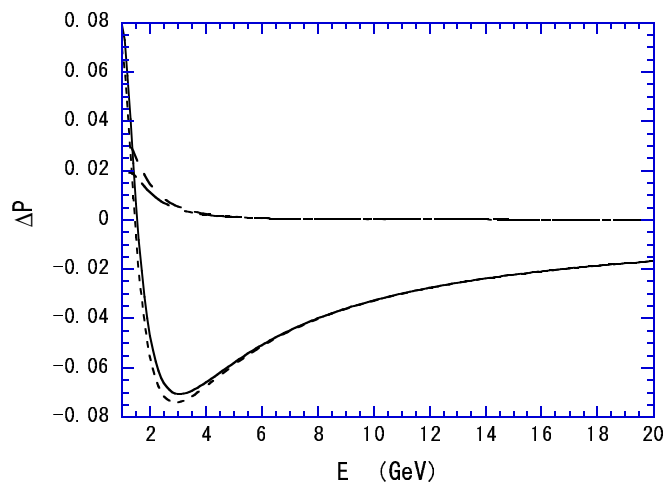


Figure 7: The CP violating effect in ν_μ oscillation at $L = 730$ km with the same parameter values as in Fig.4 except for $m_{31}^2 < 0$. The lines represent the same ones as in Fig.4 except for the line of FDN I contribution omitted.

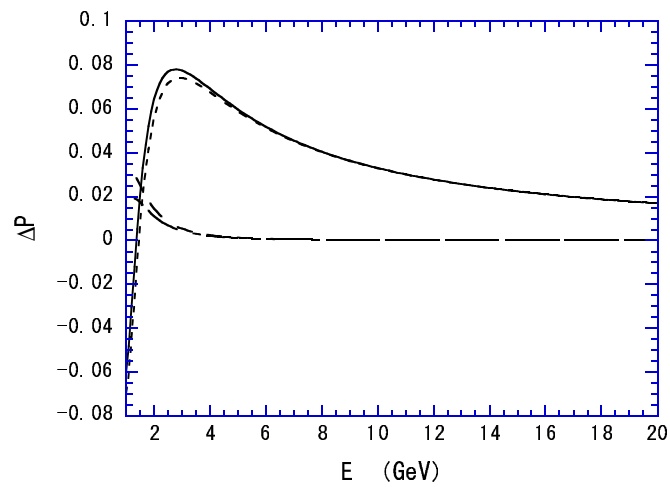


Figure 8: The CP violating effect in $\nu_\mu \rightarrow \nu_\tau$ oscillation at $L = 730$ km with the same parameter values as in Fig.4 except for $\theta_{13} = 0$ and $m_{31}^2 < 0$. The lines represent the same ones as in Fig.4 except for the line of FDN I contribution omitted.

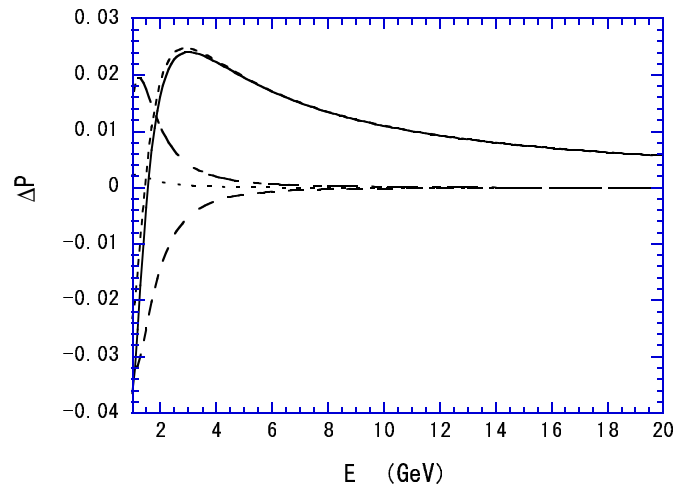


Figure 9: The CP violating effect in μ oscillation at $L = 730$ km with the same parameter values as in Fig.4 except for $\theta_{12} = 0.01$ and $\theta_{13} = 0.01$. The lines represent the same ones as in Fig.4.

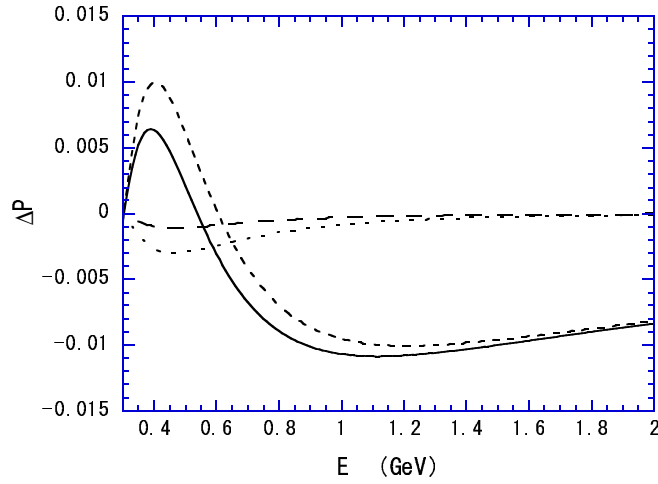


Figure 10: The CP violating effect in $\nu_{\mu} \rightarrow \nu_{\tau}$ for the neutrino energy range $E = 0.3 - 2$ GeV at $L = 300$ km, with the NSNI in the ν_{μ} sector. The long-dashed, short-dashed and dotted lines are the fake CP violating effects due to the ordinary, FCNI and FDNI matter effects, respectively. The solid line is the total CP violating effect with these three matter effects. The parameter values are $\theta_{12} = 0.03$; $\theta_{13} = 0.16$; $\theta_{23} = 0$; $s_{12} = 0.541$; $s_{23} = 0.742$; $s_{13} = 0.16$; $\delta = \pi/2$; $m_{21}^2 = 5 \times 10^5$ eV², and $m_{31}^2 = 2.5 \times 10^3$ eV² (> 0).

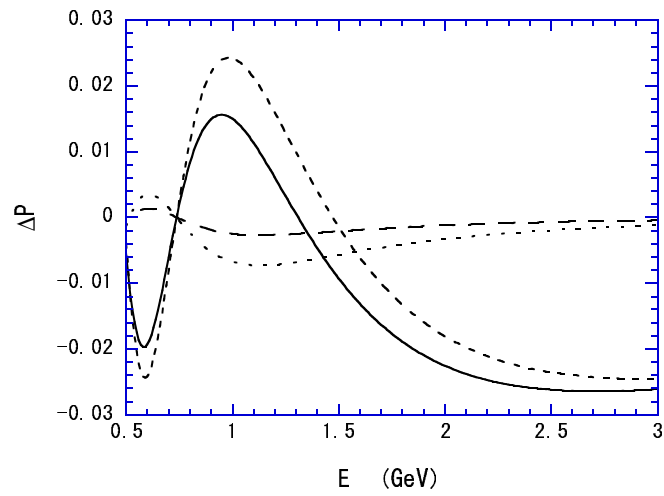


Figure 11: The CP violating effect in $\mu \rightarrow e \gamma$ for the neutrino energy range $E = 0.5 - 3.0$ GeV at $L = 730$ km with the same parameter values as in Fig.10. The lines represent the same ones as in Fig.10. The only change from Fig.10 is the baseline length.

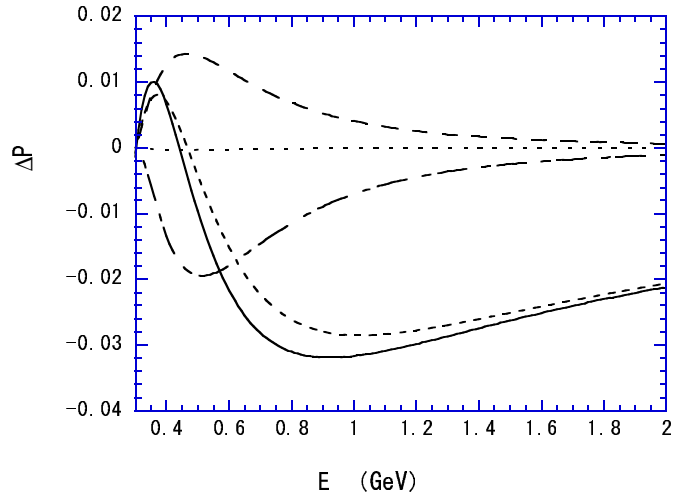


Figure 12: The CP violating effect in $\nu_e \rightarrow \nu_e$ oscillation for the neutrino energy range $E = 0.3 - 2$ GeV at $L = 300$ km, with the NSNI in ν_e sector. The dash-dotted line is the pure CP violating effect. The long-dashed, short-dashed and dotted lines are the fake CP violating effects due to the ordinary, FCNI and FDNI matter effects, respectively. The solid line is the total CP violating effect with the pure and fake ones. The parameter values are $\theta_{12} = 33^\circ$; $\theta_{13} = 9^\circ$; $\theta_{23} = 45^\circ$; $\delta = 270^\circ$; $s_{12} = 0.541$; $s_{23} = 0.742$; $s_{13} = 0.16$; $\delta = 270^\circ$; $m_{21}^2 = 5 \times 10^5 \text{ eV}^2$, and $m_{31}^2 = 2.5 \times 10^3 \text{ eV}^2 (> 0)$.

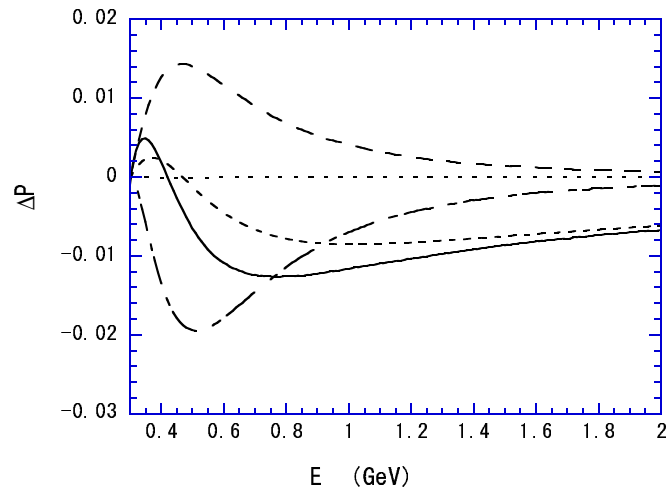


Figure 13: The CP violating effect in ν_e oscillation at $L = 300$ km with the same parameter values as in Fig.12 except for $\theta_{12} = 0.03$ and $\theta_{13} = 0.03$. The lines represent the same ones as in Fig.12.

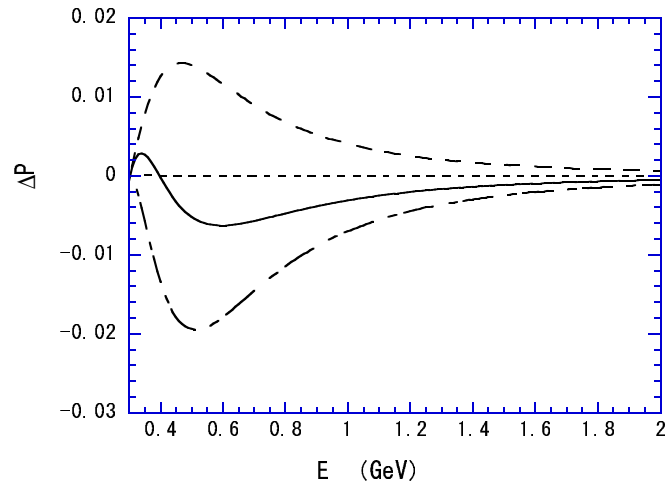


Figure 14: The CP violating effect in ν_e oscillation at $L = 300$ km with the same parameter values as in Fig.12 except for $j = 7 \times 10^5$ and $\theta = 0.01$. The lines represent the same ones as in Fig.12 except for the line of the FDN I contribution omitted.